

Fig. 2. Recursive implementations of the DFT with limited precision.

Without loss of generality, it can be assumed that $k = N$ so that

$$\begin{aligned}\widetilde{\mathbf{W}}_{N+j} &= \mathbf{W}_{N+j} - \prod_{m=0}^{j-1} (\mathbf{I} - \mathbf{R}_{N+m}) \epsilon_N \\ &= \mathbf{W}_{N+j} - \prod_{m=0}^{j-1} (\mathbf{I} - \mathbf{R}_m) \epsilon_N,\end{aligned}\quad (11)$$

where $\mathbf{R}_m \triangleq \mathbf{I} - \overline{\mathbf{X}}_m \mathbf{X}_m^T$.

As seen previously, the vectors $\{\mathbf{X}_0, \mathbf{X}_1, \dots, \mathbf{X}_{N-1}\}$ form an orthonormal basis in the N -dimensional space. Similarly, the vectors $\{\overline{\mathbf{X}}_0, \overline{\mathbf{X}}_1, \dots, \overline{\mathbf{X}}_{N-1}\}$ form another orthonormal basis in the same space. Any error vector ϵ_N can be decomposed into its N components in this last basis:

$$\epsilon_N = \sum_{n=0}^{N-1} \epsilon_N(n) \overline{\mathbf{X}}_n. \quad (12)$$

The product $\mathbf{R}_m \epsilon_N$ can then be evaluated as

$$\begin{aligned}\mathbf{R}_m \epsilon_N &= (\mathbf{I} - \overline{\mathbf{X}}_m \mathbf{X}_m^T) \epsilon_N \\ &= (\mathbf{I} - \overline{\mathbf{X}}_m \mathbf{X}_m^T) \sum_{n=0}^{N-1} \epsilon_N(n) \overline{\mathbf{X}}_n \\ &= \epsilon_N - \epsilon_N(m) \overline{\mathbf{X}}_m.\end{aligned}\quad (13)$$

The multiplication of the error by the matrix \mathbf{R}_m eliminates its m th component and leaves the other components unchanged. Multiplying the residual error vector by \mathbf{R}_{m+1} will cancel out its $(m+1)$ th component, and so on. As iterations proceed, the modulus of the error vector decreases monotonically. After N iterations, all its components have been canceled, and the error reduces to zero.

For illustrative purposes, consider the signal $x(k) = \sin(2\pi f_1 k/N) + \sin(2\pi f_2 k/N)$ and its 32-point DFT. We wrote a C program implementing the nonadaptive sliding-DFT and the LMS spectrum analyzer algorithms. To demonstrate the effect of limited precision, we rounded off to 7 b the mantissas of the floating point results of all arithmetical operations.² For comparison, we also coded the exact DFT of $x(k)$. Fig. 2 represents the sum of

²In the IEEE standard for floating point arithmetic, the mantissa occupies 23 b, the fraction 8, and the sign one).

the square modulus of the DFT components, $\sum_{i=0}^{31} |DFT_k(i)|^2$, as a function of time, for $f_1 = 0.03$ and $f_2 = 1.1$. The DFT given by the LMS spectrum analyzer practically coincides with the exact DFT. The nonrecursive sliding-DFT follows the exact DFT for a while but it eventually diverges.

V. CONCLUSION

While the nonadaptive sliding-DFT allows roundoff errors to accumulate over time, the LMS spectrum analyzer uses its adaptation loop to automatically eliminate errors in a number of iterations equal to the length of the DFT. It does not require significantly more operations per iteration than the nonadaptive sliding-DFT. These results naturally extend to other transforms once implemented adaptively (see [5] for a generalization of the LMS spectrum analyzer to other orthonormal transforms). For these reasons, we recommend the use of the LMS spectrum analyzer for any application where a sliding orthonormal transform must be performed over long trains of data.

REFERENCES

- [1] L. R. Rabiner and B. Gold, *Theory and Application of Digital Signal Processing*. Englewood Cliffs, NJ: Prentice-Hall, 1975.
- [2] B. Widrow, Ph. Baudrenghien, M. Vetterli, and P. F. Titchener, "Fundamental relations between the LMS algorithm and the DFT," *IEEE Trans. Circuits Syst.*, vol. CAS-34, no. 7, pp. 814-819, July 1987.
- [3] B. Widrow, J. M. McCool, and M. Ball, "The complex LMS algorithm," *Proc. IEEE*, vol. 63, pp. 719-720, Apr. 1975.
- [4] S. S. Narayan, A. M. Peterson, and M. J. Narasimha, "Transform domain LMS algorithm," *IEEE Trans. Acoustics, Speech, Signal Process.* vol. ASSP-31, no. 3, pp. 609-615, June 1983.
- [5] S.-S. Wang, "LMS algorithm and discrete orthogonal transforms," *IEEE Trans. Circuits Syst.*, vol. 38, no. 8, pp. 949-951, Aug. 1991.

A Class of Second-Order Integrators and Low-Pass Differentiators

Mohamad Adnan Al-Alaoui

Abstract—A novel class of stable, minimum phase, second-order, low-pass IIR digital differentiators is developed. It is obtained by inverting the transfer functions of a class of second-order integrators, stabilizing the resulting transfer functions, and compensating their magnitudes. The class of second-order integrators is obtained by interpolating the traditional Simpson and trapezoidal integrators. The resulting integrators have a perfect -90° phase over the Nyquist interval and could better approximate the ideal magnitude response than either of the two traditional integrators. In addition to the above two integrators, the Tick integrator is also a member of the class. The resulting integrators and differentiators extend the frequency range of operation beyond that possible by using either of the two traditional integrators. The low order and high accuracy of the filters make them attractive for real time applications.

I. INTRODUCTION

The basic concept came from observing that the ideal integrator response lies between the responses of the traditional trapezoidal and

Manuscript received January 20, 1994; revised November 24, 1994. This work was supported in part by the Research Board of the American University of Beirut, Beirut, Lebanon. This paper was recommended by Associate Editor I. Pitas.

The author is with the Electrical and Computer Engineering Department, The American University of Beirut, Beirut, Lebanon.

IEEE Log Number 9410007.

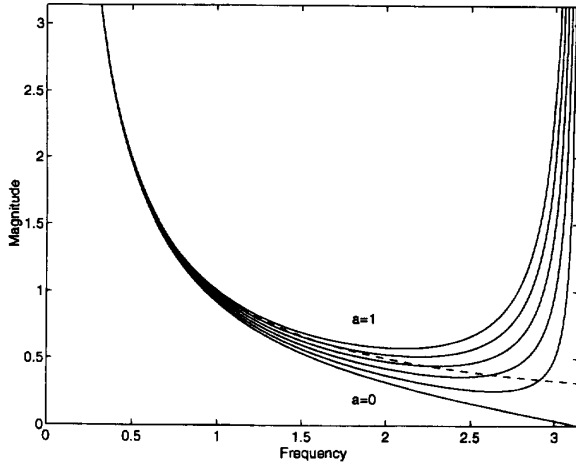


Fig. 1. The magnitude response of the class of second-order integrators for $a = 0$ to $a = 1$, with 0.2 increments (solid lines) and the magnitude response of the ideal integrator (dashed line).

Simpson integrators. Thus it seems reasonable that interpolating the above two rules could yield integrators that better approximate the ideal integrator.

II. NONMINIMUM PHASE DIGITAL INTEGRATORS

It was shown in [1] and [2] that the magnitude of the frequency response of the ideal integrator lies between the Simpson and the trapezoidal integrators. Interpolating the two integrators in a manner similar to that in [2] and [3] and to that used to obtain the Simpson rule from the midpoint and trapezoidal rule [4] yields

$$H(z) = aH_S(z) + (1-a)H_T(z), \quad 0 \leq a \leq 1 \quad (1)$$

where a is a real valued parameter defined on the closed interval $[0, 1]$. $H_S(z)$ and $H_T(z)$ are the transfer functions of the Simpsons and the trapezoidal integrators, respectively, and are shown below:

$$H_S(z) = \frac{T(z^2 + 4z + 1)}{3(z^2 - 1)} \quad (2)$$

$$H_T(z) = \frac{T(z + 1)}{2(z - 1)} \quad (3)$$

Substituting (2) and (3) in (1) and simplifying yields the following transfer function for the novel class of nonminimum phase integrators:

$$H(z) = \frac{T(3-a)\{z^2 + [2(3+a)/(3-a)]z + 1\}}{6(z^2 - 1)} \quad (4)$$

The numerator of (4) may be factored to yield

$$H(z) = \frac{T(3-a)[(z + r_1)(z + r_2)]}{6(z^2 - 1)} \quad (5)$$

where

$$r_1 = \frac{(3+a+2\sqrt{3a})}{(3-a)}; \quad \text{and} \quad r_2 = \frac{(3+a-2\sqrt{3a})}{(3-a)} \quad (6)$$

This class of integrators has the property that its zeros are reciprocal pairs around the unit circle in the z -plane, since $r_1 = 1/r_2$. Note that this property is shared by the Tick integrator [1], [5]. Indeed (4) reduces to the Tick integrator when $a = 0.8495$.

With $z = e^{j\omega}$, the magnitude response is given by the following equation:

$$|H(e^{j\omega})| = [T(3-a)(1 + 2r_1 \cos \omega + r_1^2)^{1/2} \cdot (1 + 2r_2 \cos \omega + r_2^2)^{1/2}] / [12|\sin \omega|] \quad (7)$$

TABLE I
MAXIMUM VALUES OF RELATIVE PERCENTAGE ERRORS AND THE CORRESPONDING RANGES OF THE INTEGRATORS AND DIFFERENTIATORS AS a IS VARIED

a	Relative % error	Range as a fraction of the Nyquist frequency
1 (Simpson)	0.0053	0 - 0.1
1 (Simpson)	1.7	0 - 0.4
0.9	0.3	0 - 0.4
0.9	2	0 - 0.5
0.85 (Tick)	1	0 - 0.5
0.85 (Tick)	5	0 - 0.6
0.78	2	0 - 0.6
0.7	3.2	0 - 0.6
0.7	7	0 - 0.7
0.65	4.5	0 - 0.7
0.5	10	0 - 0.8
0 (Trapezoidal)	13.5	0 - 0.4
0 (Trapezoidal)	2	0 - 0.15

Fig. 1 shows the magnitude responses for the new class of integrators, for $a = 0$ to $a = 1$ with 0.2 increments, together with that of the ideal integrator. For any value of a , the error in the magnitude response is zero at zero frequency. The results are summarized in Table I. If it is not important to have zero error at zero frequency, then allowing equal absolute values of extremum errors, the percent error values reported above could be reduced [3]. The new integrators could give higher accuracy and/or greater range of frequencies than either of the constituent traditional integrators. Additionally the phase of the resulting class of integrators is exactly -90° over the entire Nyquist frequency range.

Note that the value $T = 1$ is used in the frequency plots shown in Fig. 1 and the Nyquist frequency is π rad/sec. In subsequent figures the Nyquist frequency range will be normalized to 1.

After developing the above class of integrators as shown above, it became evident that this is the same class of integrators developed by Tick and generalized by Hamming [1, pp. 241-244]. The new derivation provides further insight into the properties of this class of integrators. For example, neither Tick nor Hamming realized that the trapezoidal integrator is a member of the class or that a linear input would also be integrated correctly.

Tick obtained the following difference equation

$$y(n+1) = y(n-1) + \alpha x(n+1) + \beta x(n) + \alpha x(n-1) \quad (8)$$

where x and y represent the input and output, respectively. Tick required that a constant input should be integrated correctly which results in the relation $\beta = 2 - 2\alpha$. Thus, the above difference equation would have one free parameter and it can be shown to be the same as the difference equation obtained from (4) with $T = 1$ and $a = 3\beta - 3 = 3 - 6\alpha$. Tick also required the frequency magnitude error curve to be Chebyshev in the lower half of the Nyquist interval resulting in $\alpha = 0.35785$ which corresponds to $a = 0.8529$. He, however, carried out further refinements, by leveling the error curve through repeated computations, and obtained $\alpha = 0.3584$ which corresponds to $a = 0.8496$.

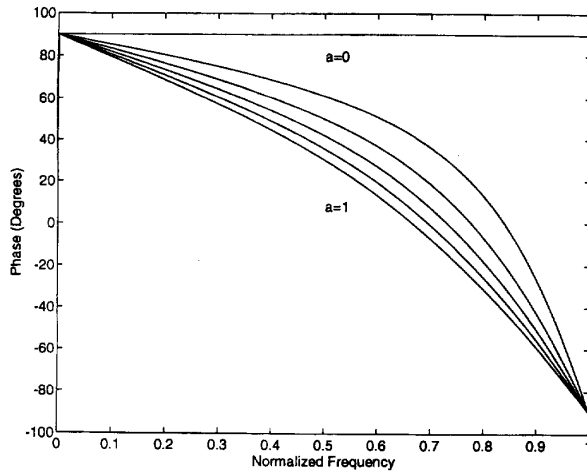


Fig. 2. The phase response of the new differentiators for $a = 0$ to $a = 1$ with 0.2 increments.

III. A CLASS OF SECOND-ORDER DIGITAL LOW-PASS DIFFERENTIATORS

The following transfer function for a class of stable, minimum phase, low-pass differentiators is obtained by applying the approach outlined in [5] to (4), and noting that $r_2 = 1/r_1$:

$$G(z) = \frac{6(z^2 - 1)}{Tr_1(3 - a)(z + r_2)^2}. \quad (9)$$

The approach developed in [5], and applied in [2] and [6], consists of inverting the transfer function of an integrator, stabilizing the resulting transfer function by reflecting the poles that lie outside the unit circle in the z -plane to inside the unit circle, and compensating the magnitude appropriately. The compensation notes that if a pole that lies at a radius r is replaced by a pole that lies at a radius of $1/r$, the magnitude of the resulting transfer function will be multiplied by r . Thus to compensate for the change in magnitude, the resulting transfer function should be multiplied by $1/r$. The magnitude of the frequency response of the resulting differentiator has the same range and accuracy as the integrator.

Fig. 2 shows the phase responses for the resulting low-pass differentiators for $a = 0$ to 1 with 0.2 increments. The resulting phase responses are almost linear over the passbands.

Fig. 3 shows the minimax differentiators corresponding to the minimax integrators reported by Hamming. Table II shows the maximum errors of the minimax differentiators, or integrators, over the corresponding lowest fraction of the Nyquist interval. The values of λ are taken from 0 to 1 with 0.1 increments in addition to the value of 0.05.

The resulting low-pass differentiators compare favorably with the 10 point low-pass differentiator reported by Oppenheim and Schaffer which has an error of about 12 percent for a range of 0.8 of the Nyquist frequency [7]. This is clearly bettered by some of the differentiators listed in Tables I and II, in addition of course to the smaller delay introduced by the new class of differentiators. The differentiators of Kumar and Dutta Roy could exhibit impressive accuracies [8]. They report a relative error of less than -160 dB for a nine point low-pass differentiator in the range from 0 to 0.05 of the Nyquist frequency. Applying the minimax design with a range of 0.05 of the Nyquist frequency to the new class of differentiators yields $a = 0.9984$ and a respectable relative error of -127 dB which

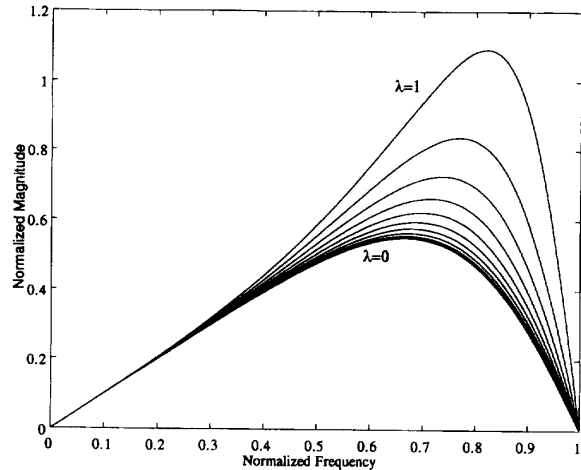


Fig. 3. The magnitude responses of the minimax differentiators for $\lambda = 0$ to $\lambda = 1$ with 0.1 increments, where λ is the fraction of the Nyquist frequency.

TABLE II
MAXIMUM VALUES OF THE RELATIVE PERCENTAGE ERRORS AND THE CORRESPONDING RANGES OF THE MINIMAX INTEGRATORS AND DIFFERENTIATORS AS λ IS VARIED, WHERE λ IS THE FRACTION OF THE NYQUIST FREQUENCY

λ	a	Absolute value of Maximum Relative % error	Range as a fraction of the Nyquist frequency
0	1	0.0004	0 - 0.05
0.05	0.9984	0.00004241	0 - 0.05
0.1	0.9945	0.0009	0 - 0.1
0.2	0.9778	0.0155	0 - 0.2
0.3	0.9494	0.0815	0 - 0.3
0.4	0.9083	0.2904	0 - 0.4
0.5	0.8529	0.8366	0 - 0.5
0.6	0.7813	2.1556	0 - 0.6
0.7	0.6904	5.2694	0 - 0.7
0.8	0.5764	12.9057	0 - 0.8
0.9	0.4337	33.4180	0 - 0.9
1	0.2594	98.8424	0 - 1

makes it, with the smaller delay, an attractive alternative for real time applications.

IV. CONCLUSION

A class of second-order integrators is obtained by interpolating two extreme cases, namely the traditional Simpson and trapezoidal integrators. The resulting integrators better approximate the magnitude characteristics of the ideal integrator by widening the frequency range where the desired response is captured as compared to the two traditional integrators. The integrators integrate constant and linear inputs exactly and exhibit perfect phase over the entire Nyquist interval. Additionally there is one free parameter that can be adjusted by imposing an appropriate constraint.

The paper develops a new class of stable second-order low-pass differentiators. The low-pass differentiators have the desirable magnitude response of zero at zero frequency and at the Nyquist frequency. In addition a free parameter could be adjusted by imposing an appropriate constraint. A set of minimax differentiators, and integrators, is obtained by minimizing the maximum magnitude error in the lowest λ th fraction of the Nyquist interval. The phases of the resulting differentiators are almost linear over the frequency ranges of interest. The low orders and high accuracies of the integrators and differentiators make them attractive for real time applications.

ACKNOWLEDGMENT

The author would like to thank C. L. Nikias for providing the atmosphere conducive to research by inviting him to spend the summer of 1993 at the USC Signal and Image Processing Institute, where this research was carried out. He is also grateful to G. A. Tsihrintzis, C.-Y. Tseng, and Y. Chen of USC for their help in the production of the manuscript.

REFERENCES

- [1] R. W. Hamming, *Digital Filters*, 3rd ed. Englewood Cliffs, NJ: Prentice-Hall, 1989.
- [2] M. A. Al-Alaoui, "Novel digital integrator and differentiator," *Electron. Lett.*, vol. 29, no. 4, pp. 376–378, 1993. (See also *ERRATA*, *Electron. Lett.*, vol. 29, no. 10, pp. 934, 1993).
- [3] J. Le Bihan, "Novel class of digital integrators and differentiators," *Electron. Lett.*, vol. 29, no. 11, pp. 971–973, 1993.
- [4] G. E. Forsythe, M. A. Malcolm, and C. V. Moler, *Computer Methods for Mathematical Computations*. Englewood Cliffs, NJ: Prentice-Hall, 1989, ch. 5.
- [5] M. A. Al-Alaoui, "Novel approach to designing digital differentiators," *Electron. Lett.*, vol. 28, no. 15, pp. 1376–1378, 1992.
- [6] ———, "Novel IIR differentiator from the Simpson integration rule," *IEEE Trans. Circuits Syst. I*, vol. 41, no. 2, pp. 186–187, Feb. 1994.
- [7] A. V. Oppenheim and R. W. Schaffer, *Discrete-Time Signal Processing*. Englewood Cliffs, NJ: Prentice-Hall, 1989.
- [8] B. Kumar and S. C. Dutta-Roy, "Design of digital differentiator for low frequencies," *Proc. IEEE*, vol. 76, no. 3, pp. 287–289, Mar. 1988.

A Rational Complex Frequency Domain Model for the Completely Transposed Transmission Line with Initial Voltage and Current Distributions

Jung-Chien Li

Abstract—The transmission-line equations for a completely transposed transmission line are decoupled so that the Laplace transformation can be applied for each phase sequence. We then obtain the equivalent two-port admittance matrix with current generators connected to the transmission-line terminals which account for the initial voltage and current distributions. This circuit model is suitable for power network analysis and can be rationalized so that analytical time-domain waveforms can be obtained by applying the Heaviside partial fraction expansion method in Laplace inversion. The three sequence networks can be combined to give the relation between phase voltages and phase currents when this transmission line is embedded in an unbalanced power network.

I. INTRODUCTION

In the transient analysis of a transmission line, the initial voltage and current distributions (known as the initial conditions) are usually neglected [1]–[3]. However, the initial conditions contribute to the transient component of the circuit response and should not be ignored, especially when the transmission network has just been switched from a different topological state which produced voltage and current distributions on the examined transmission line. The effects of arbitrary initial voltage and current distributions on a lossy signal transmission line were considered in [4] and [5].

This paper investigates the three-phase completely transposed transmission line, which is normally encountered in power transmission. Since it is a balanced network, the transmission-line equations can be easily decoupled to give three independent sets of equations, each of which relate to the zero, positive, and negative sequences, respectively. This simplifies the solving procedure and the equivalent circuit for each phase sequence is easily obtained. The three sequence networks can be combined to give the relation between phase voltages and phase currents when this transmission line is embedded in an unbalanced power network.

II. DECOUPLING THE TRANSMISSION-LINE EQUATIONS

In a three-phase transmission line of length l , the phase voltages $v(x, t)$ and the phase currents $i(x, t)$ can be described by the well-known transmission-line equations, which can be Laplace transformed (with respect to t) to give

$$-\frac{dV(x, s)}{dx} = (sL + R)I(x, s) - Li_0(x) \quad (1)$$

$$-\frac{dI(x, s)}{dx} = (sC + G)V(x, s) - Cv_0(x) \quad (2)$$

where

$$v_0(x) = v(x, t = 0) = \sum_{k=0}^{\infty} \beta_k \cos \frac{k\pi x}{l} \quad (3)$$

$$i_0(x) = i(x, t = 0) = \sum_{k=0}^{\infty} \alpha_k \cos \frac{k\pi x}{l} \quad (4)$$

Manuscript received March 7, 1994; revised December 8, 1994. This paper was recommended by Associate Editor M. Tanaka.

The author is with Department of Electrical Engineering, National Taiwan Ocean University, Keelung, Taiwan, R.O.C.

IEEE Log Number 9410006.